

Functional and Pharmacological Evaluation of a Novel SCN2A Variant Linked to Early-onset Epilepsy

Scott K. Adney, John J. Millichap, Jean-Marc DeKeyser, Tatiana Abramova,
Christopher H. Thompson, and Alfred L. George, Jr.

SUPPLEMENTAL INFORMATION

1. Supplemental Figures

- Fig. S1 Functional properties of M1879T channels in either the Nav1.2 neonatal or adult splice variants.
- Fig. S2 Time dependence of resurgent current in WT and M1879T Nav1.2 channels.
- Fig. S3 Effects of carbamazepine on WT Nav1.2 channels.
- Fig. S4 Effect of carbamazepine on resurgent current.

2. Supplemental Tables

- Table S1 Atomic contacts of Met-1879 from WT and Thr-1879 from M1879T model
- Table S2 Atomic contacts of Arg-1882 from WT and Gln-1882 from R1882Q model

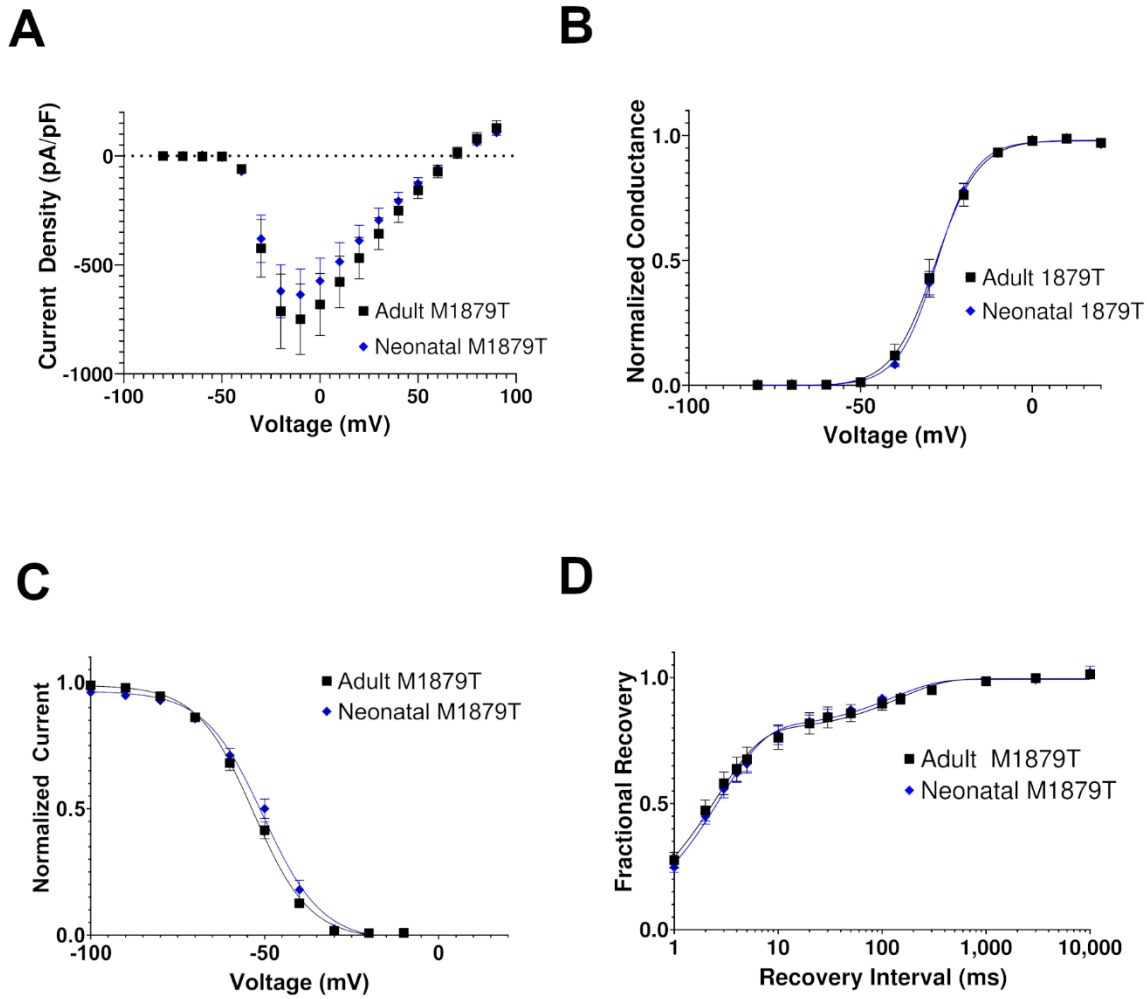


Fig. S1. Functional properties of M1879T channels in either the Nav1.2 neonatal or adult splice variant.

(A) Current density-voltage plot of adult ($n=8$) and neonatal ($n=15$) isoforms of M1879T. (B) Voltage-dependence of activation for adult ($n=14$) and neonatal ($n=12$) isoforms of M1879T. No significant differences were observed between $V_{1/2}$ values (see Table 1). (C) Voltage-dependence of inactivation for adult ($n=25$) and neonatal ($n=15$) isoforms of M1879T. No significant differences were observed between $V_{1/2}$ values. (D) Logarithmic plot of the time course of recovery from inactivation comparing adult ($n=10$) and neonatal ($n=11$) isoforms of M1879T.

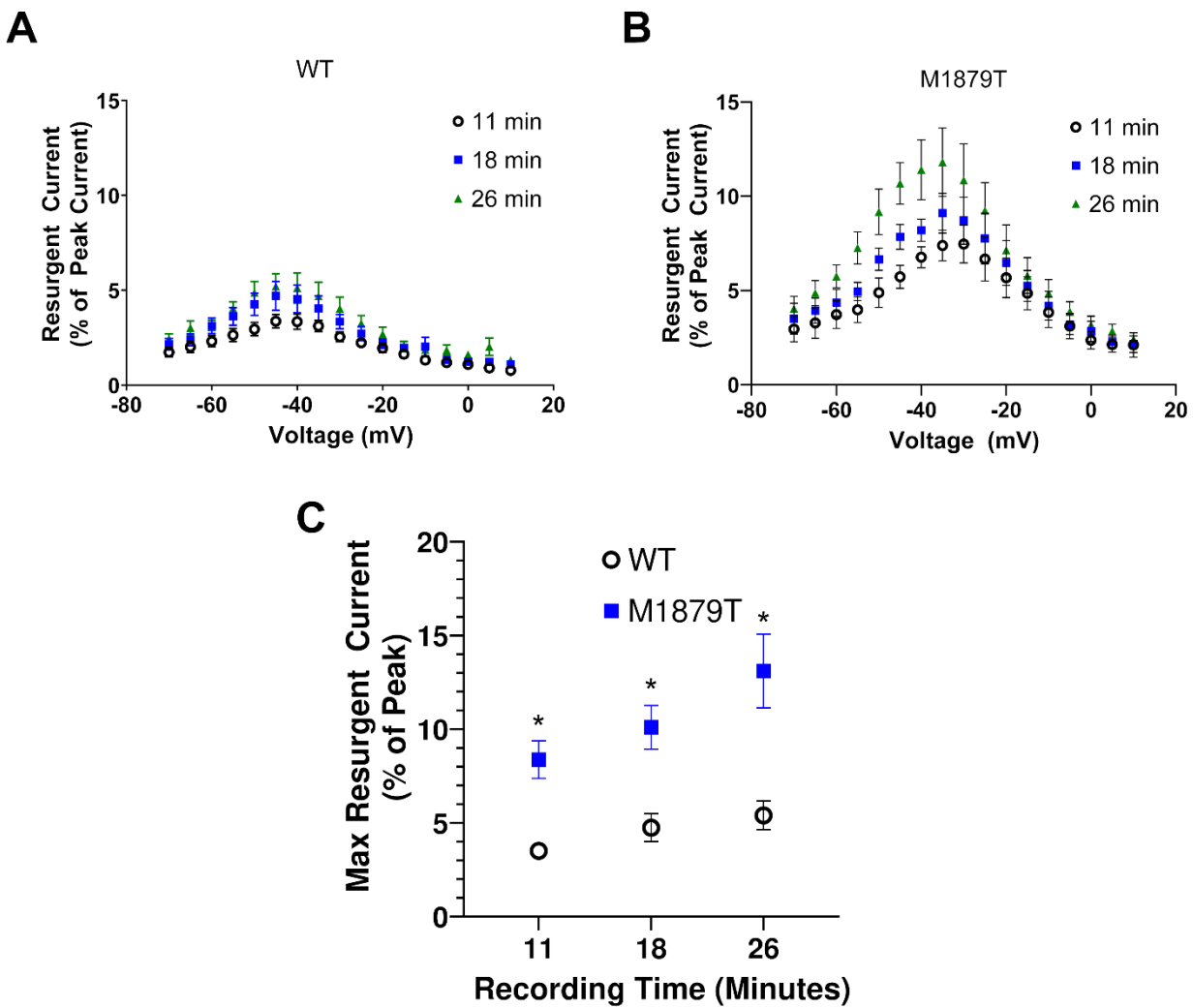


Fig. S2. Time dependence of resurgent current in WT and M1879T Nav1.2 channels.

(A) Voltage-dependence of WT NaV1.2 resurgent current (as % of peak current) at three different recording time-points. (B) Voltage-dependence of M1897T NaV1.2 resurgent current at the same three recording time-points. (C) Summary plot showing peak resurgent current (as % of peak current) at each time point for WT ($n=6$) and M1879T ($n=7$) channels. *, $p<0.05$ by Mann-Whitney U test.

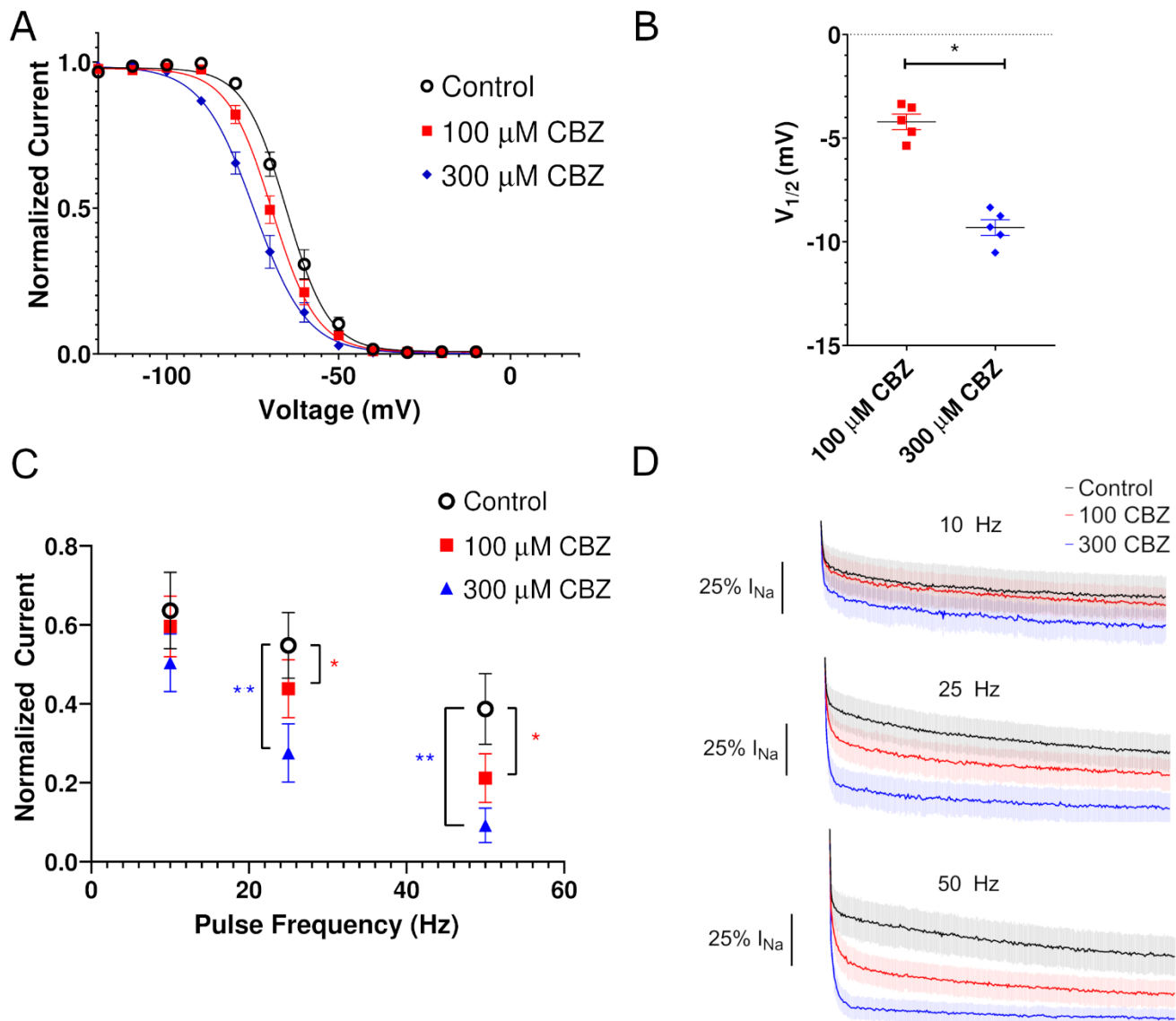


Fig. S3. Effects of carbamazepine on WT Nav1.2 channels.

(A) Carbamazepine (CBZ) induces a hyperpolarizing shift of the voltage-dependence of inactivation ($n=5$). (B) Plot of change in inactivation $V_{1/2}$ in response to 100 μ M and 300 μ M carbamazepine ($n=5$; *, $p<0.05$ by paired t-test). (C) Plot of residual current (comparing 300th pulse to 1st pulse) after 0 mV pulses at the indicated frequency with a holding potential of -90 mV. There was a significant difference in residual current at 100 μ M (*) and 300 μ M (**) at 25 Hz and 50 Hz compared to the control value ($p<0.05$, one-way ANOVA with repeated measures and Dunnett's post-hoc test, $n=5$). (D) Average time-course of CBZ treated cells at 10 Hz (top), 25 Hz (middle), and 50 Hz (bottom). The shaded area indicates the SEM.

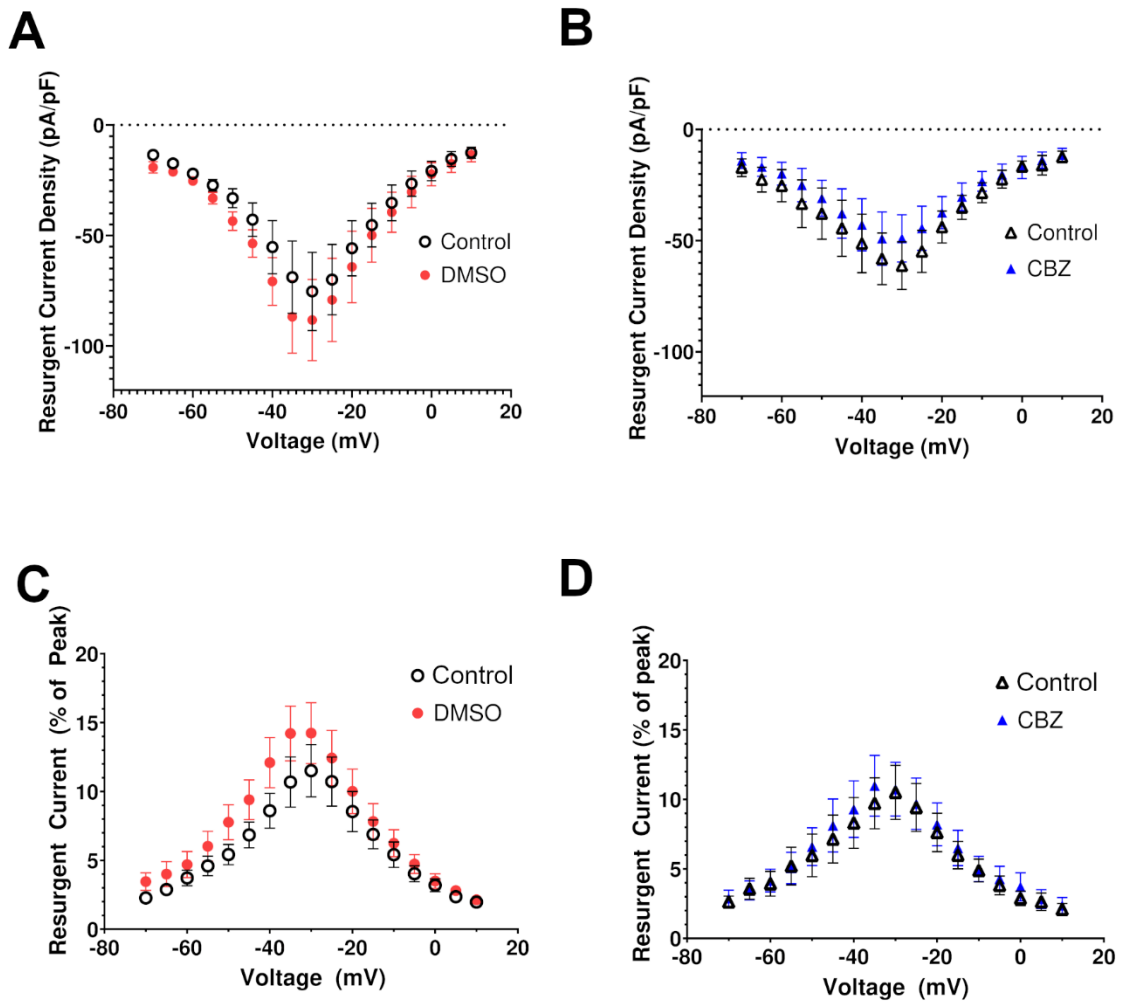


Fig. S4. Effect of carbamazepine on resurgent current.

(A) Voltage-dependence of resurgent current density in the control condition and after DMSO (vehicle) treatment ($n=7$). (B) Voltage-dependence of resurgent current density in the control condition and after 300 μ M CBZ treatment ($n=7$). (C) Resurgent current as percentage of peak vs. voltage in control and after 300 μ M CBZ treatment ($n=7$).

Table S1. Atomic contacts of Met-1879 from WT and Thr-1879 from M1879T model

Met-1879: 15 contacts			
Atom1	Atom2	Overlap	Distance
MET 1879.B CE	LEU 1875.B CG	0.275	3.485
MET 1879.B CE	THR 1862.B CG2	0.255	3.505
MET 1879.B CE	THR 1862.B OG1	0.197	3.143
MET 1879.B CG	LEU 1875.B O	0.164	3.136
MET 1879.B CE	THR 1862.B CB	0.142	3.618
MET 1879.B CE	LEU 1875.B CD2	0.132	3.628
MET 1879.B CE	PHE 1795.B CE1	0.061	3.579
MET 1879.B SD	LEU 1875.B O	-0.15	3.34
MET 1879.B CB	PHE 1859.B CE1	-0.168	3.808
MET 1879.B CB	LEU 1875.B O	-0.184	3.484
MET 1879.B CE	PHE 1795.B CZ	-0.215	3.855
MET 1879.B CE	LEU 1875.B CD1	-0.287	4.047
MET 1879.B SD	PHE 1859.B CD1	-0.298	3.828
MET 1879.B SD	LEU 1875.B CG	-0.306	3.956
MET 1879.B SD	ARG 1876.B CA	-0.343	3.993
Thr-1879: 6 contacts			
THR 1879.B CG2	LEU 1858.B CD1	0.434	3.326
THR 1879.B OG1	LEU 1875.B O	0.193	2.687
THR 1879.B CG2	LEU 1855.B CD1	0.112	3.648
THR 1879.B CB	LEU 1875.B O	-0.056	3.356
THR 1879.B CB	PHE 1859.B CE1	-0.271	3.911
THR 1879.B CG2	PHE 1859.B CE1	-0.38	4.02

Table S2. Atomic contacts of Arg-1882 from WT and Gln-1882 from R1882Q model

Arg-1882: 12 contacts			
Atom1	Atom2	Overlap	Distance
ARG 1882.B NH1	GLU 1792.B OE2	0.382	2.678
ARG 1882.B NH1	GLU 1792.B CD	0.37	3.15
ARG 1882.B CG	GLN 1878.B O	0.239	3.061
ARG 1882.B NH1	GLU 1792.B OE1	0.188	2.872
ARG 1882.B NH2	GLU 1792.B OE1	0.159	2.901
ARG 1882.B NH2	GLN 1878.B OE1	0.096	2.964
ARG 1882.B CB	GLN 1878.B O	0.08	3.22
ARG 1882.B CD	GLN 1878.B O	-0.108	3.408
ARG 1882.B NH2	GLU 1792.B CD	-0.227	3.747
ARG 1882.B CZ	GLU 1792.B OE1	-0.301	3.331
ARG 1882.B NE	GLN 1878.B OE1	-0.319	3.379
ARG 1882.B CZ	GLU 1792.B CD	-0.363	3.853
Gln-1882: 2 contacts			
GLN 1882.B CG	GLN 1878.B O	0.128	3.172
GLN 1882.B CB	GLN 1878.B O	-0.02	3.32